Texila International Journal of Public Health
Special Issue 2023
DOI: 10.21522/TIJPH.2013.SE.23.01.Art009

Fabrication, Characterization, Antibacterial and Biocompatibility Studies of Graphene Oxide Loaded Alginate Chitosan Scaffolds for Potential Biomedical Applications

Katheeja Rilah, V. Vishnu Priya*, R. Gayathri, Kavitha.S
Department of Biochemistry, Saveetha Dental College and Hospitals, Saveetha Institute of Medical and Technical Sciences, Saveetha University, Chennai, India

Abstract

Graphene oxide nanomaterial possesses greater biocompatibility. Chitosan alginate is produced from chitin by deacetylation, it is a biodegradable and biocompatible biomaterial. Graphene has a large specific surface area that enhances the antibacterial effect by enabling biocompatible interactions with bacterial membranes. To fabricate a biocompatible graphene oxide loaded alginate chitosan scaffold for potential biomedical uses and perform the characterization, antibacterial, and biocompatibility properties of ALG-CHI-GO scaffolds. The scaffolds were prepared by mixing the solution of ChitosanHCl (5 %) and graphene oxide-oxidized alginate (10 %). This gelled mixture is freeze-dried (lyophilization) to form the scaffold and is later characterized using FTIR and SEM, The scaffolds were then tested for in biocompatibility towards peripheral blood mononuclear cells and antibacterial properties against Enterococcus faecalis and Streptococcus mutans. The biocompatibility towards peripheral blood mononuclear was checked using the annexin V PI assay. To conclude that the fabricated Graphene oxide loaded chitosan alginate scaffold was found to be biocompatible and showed antibacterial properties.

Keywords: *Antibacterial activity, Biocompatibility, Chitosan alginate scaffolds, Graphene oxide*.

Introduction

The method of using suitable biomaterials to restore the biological function of injured tissues is known as skin tissue engineering [1, 2]. To guard against infections, dehydration, and consequent tissue damage [3–5], an optimal skin tissue engineering material should have a high liquid-absorbing capacity, adequate gas permeability, biocompatibility, and antibacterial characteristics In the last ten years, a wide range of biomaterials, including electrospun nanofibrous scaffolds, nanoparticles, sponges, hydrogels, and more, have been employed to heal skin tissue [6–8]. Among the various materials, natural biomedical materials have drawn a lot of interest in skin tissue engineering, because of their great biocompatibility characteristics [9]. Due to its unique qualities like biodegradability, biocompatibility, nontoxicity, accelerated wound healing, and excellent sterilization properties, chitosan (CS), one of the most alluring substances, has garnered considerable attention and it does not readily cause syneresis [10, 11]. Alginate (Alg) is a naturally occurring polysaccharide polymer with a highly hydrophilic characteristic obtained from algae or seaweed. It is extensively utilized in biomedical applications as a thickening, coagulant, and dispersion, particularly in wound dressings [12, 13]. Other advantages include biodegradability, simple removal from the body, highly porous with interconnected spaces favorable for the diffusion of gasses and nutrients to cells and the migration of many cells [14].

Received: 19.12.2023 ***Accepted: 23.12.2023*** ***Published on: 30.12.2023***

****Corresponding Author: vishnupriya@saveetha.com***

Graphene oxide (GO) has emerged as a promising nanomaterial for various electronics, biomedicine, energy, environment, and biotechnology applications in recent years [15]. Many studies on GO demonstrated their antibacterial effects against different bacterial strains, including Gram-positive and Gram-negative bacteria [16] In this study, we have fabricated a graphene oxide-loaded alginate chitosan scaffold (ALG-CHI-GO) and investigated their biocompatibility and antibacterial properties.

Experimental Section

Preparation of Chitosan HCl and Oxidized Alginate

ChitHCl was prepared by the method reported earlier [17]. About 10 g of chitosan was dispersed in 100 mL of 60% ethanolic HCl and stirred magnetically for 3 h at 20 ℃. The suspension was centrifuged, and the precipitate was washed extensively with the acetone-water mixture (6:2) and dialyzed against milli Q water until the dialysate reached neutral pH. The product was then freeze-dried and stored at 4 ℃ until use.

The oxidation of sodium alginate was carried out by a procedure as reported earlier [18]. About 220 mg of sodium *m*-periodate was added into 10 mL of a 10% sodium alginate solution and stirred under dark for 6h. After stirring, the reaction was arrested by adding a few drops of ethylene glycol. The contents were then dialyzed against water for two days by frequently changing the water. The solution was then frozen, lyophilized to dryness, and stored in the desiccator until use.

Preparation of ALG-CHI-GO Scaffolds

The scaffolds were prepared using the earlier method [17]. About 500 µl of 5 % chitosan HCl was added to a 10 % solution of oxidized alginate with graphene oxide. This mixture is freeze-dried (lyophilization) to form the scaffold and is later characterized using various instruments Figure 1 shows the lyophilized scaffold.

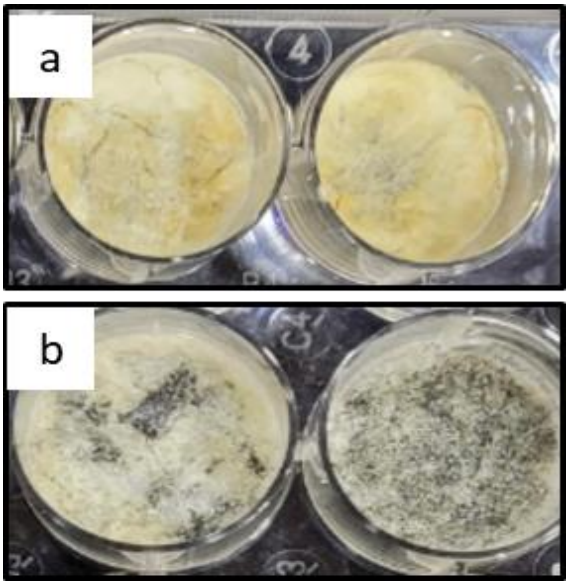

Figure 1. Lyophilized Scaffolds of (a) ALG-CHI and (b) ALG-CHI-GO

Characterization Studies

The functional groups present in the ALG-CHI scaffold and ALG-CHI-GO scaffold were investigated using Fourier transform infrared spectroscopy (FTIR) in the range of 3500 - 500 cm^{-1}. The size and structural morphology of ALG-CHI-GO were analyzed using a Scanning electron microscope (SEM) [19]. The water contact angle of the scaffolds was measured to test the hydrophilicity of the scaffolds [20].

Antibacterial Studies

Antibacterial effect of the ALG-CHI-GO against two different bacterial strains *Enterococcus faecalis* and *Streptococcus mutans* was performed using Tube assay method [21, 22]. More briefly, serial dilutions (0.39 - 100 μg/mL) of the ALG-CHI-GO were prepared for the study. A sterile 1.5 mL tube was set up with *S. mutans* and *Enterococcus faecalis* separately. Tube 1 contains control strains. Tubes 9-10 contain the serial dilution of ALG-CHI-GO mixed with sloppy agar and the test organisms. All the tube contents were thoroughly mixed using the sterile micropipette, and the plates were incubated at 30°C for 18 h. The lowest concentration with no visible growth of *Enterococcus faecalis* and *Streptococcus mutans* was recorded as MIC.

Annexin V PI Assay

To check the biocompatibility of developed ALG-CHI-GO, an annexin V PI assay was carried out. Following the approval from the institutional ethical committee, blood was collected from healthy donors. An equal volume of blood was added over histopaque and centrifuged in gradient centrifuge at 2000 rpm for 30 minutes to isolate Peripheral blood mononuclear cells (PBMCs). Buffy coat obtained after centrifugation was cultured in RPMI media containing 10% Fetal Bovine serum (FBS), 1% amino acid L-glutamine, 1% Penstrep. 100 µl of ALG-CHI-GO was added to the above culturing cells and the culturing was done in triplicate for 12 h. Cells without ALG-CHI-GO were taken as control. The cultured cells were collected and stained. For staining 5µl of Annexin V and 5µl of propidium iodide was added and kept at room temperature for 15 minutes.

After incubation, 400 µL of 1X binding buffer was added to all tubes and observed for apoptosis using BD FACS Lyric flow cytometry. Result analysis was done using FACSuite 4.1 software [23].

Results

Characterization of Scaffolds

Figure 2 represents the FTIR of ALG-CHI and ALG-CHI-GO scaffolds. In the ALG-CHI scaffold, the intense peaks were 3266, 2915, 2361, 1602, 1410, 1319, 1148, 1024, 816 and 558 cm^{-1}. The peak 3266 cm^{-1} corresponds to O-H / N-H / C-H stretching, indicating the presence of carboxylic acid / secondary amine/alkyne group. 2915 cm^{-1} corresponds to C-H stretching, indicating an alkane group. 1602 cm^{-1} corresponds to C=C stretching / N-H bending, indicating conjugated alkene/amine / cyclic alkene.1410 cm^{-1} corresponds to O-H bending / S=O stretching, indicating the carboxylic acid/alcohol/sulfate/sulfonyl chloride group. 1319 cm^{-1} corresponds to O-H bending, indicating phenol group. 1148 cm^{-1} corresponds to C-O stretching, indicating a tertiary alcohol / aliphatic ether group. 1024 cm^{-1} corresponds to S=O stretching, indicating the sulfoxide group. 816 cm^{-1} corresponds to C-Cl stretching / C=C bending, indicating the halo compounds/alkene group. 558 cm^{-1} corresponds to C-Cl / C-Br / C-l stretching indicating halo compounds. Similarly, the FTIR of the ALG-CHI-GO scaffold gave intense peaks at 3239, 1620, 1522, 1382, 1149, 1062, 1020, 640, 545 and 517 cm^{-1}. The peak at 3239 cm^{-1} corresponds to O-H stretching, indicating the carboxylic acid group. 1620 cm^{-1} corresponds to C=C stretching / N-H bending / C-C stretching / C=C stretching, indicating conjugated alkene/amine / cyclic alkene / α, β-unsaturated ketone group. 1522 cm^{-1} corresponds to N-O stretching indicating the nitro compound. 1382 cm^{-1} corresponds to CH bending, indicating the aldehyde/alkane group. 1149 cm^{-1} corresponds to C-N stretching / C-O stretching, indicating an amine / aliphatic ether group. 1062 cm^{-1} corresponds to C-O stretching / S=O stretching, indicating the primary alcohol/sulfoxide group.1020 cm^{-1} corresponds to C-N stretching, indicating an amine group. 640 cm^{-1} corresponds to C-Cl / C-Br stretching, indicating a halo compound. 545 and 517 cm^{-1}

correspond to C-Br / C-l stretching, indicating halo compound. This analysis showed that various functional groups are involved in the fabrication of ALG-CHI-GO scaffolds.

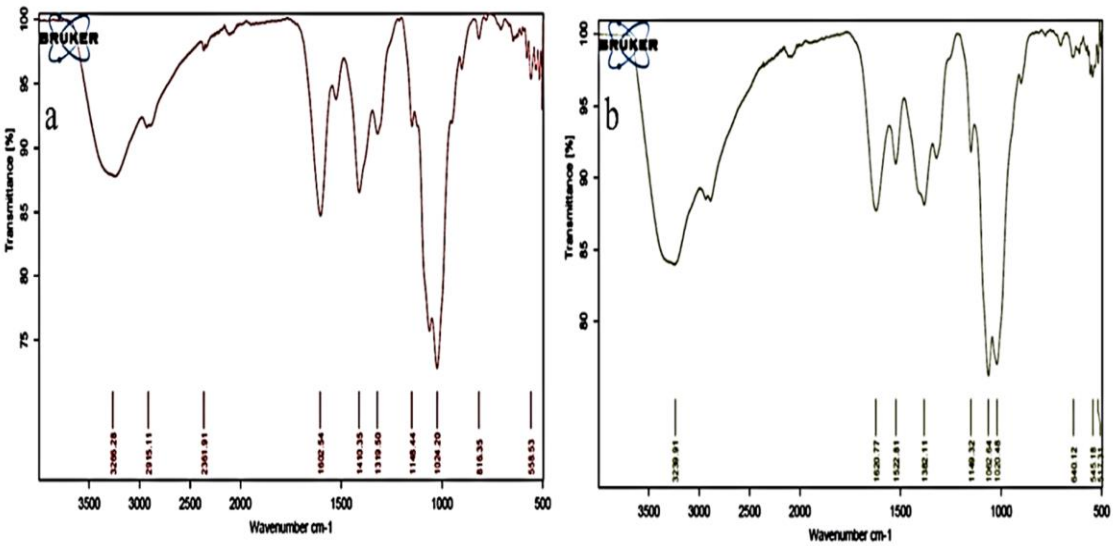

Figure 2. FTIR spectra of ALG-CHI (a) and ALG-CHI-GO (a) Scaffold

The SEM analysis revealed the porous structure of the graphene oxide-loaded alginate chitosan scaffold. Figure 3 represents the SEM images of the ALG-CHI scaffold and ALG-CHI-GO scaffold.

The water contact angle measurement is depicted in Figure 4. The results showed an average angle of 38.13 degrees.

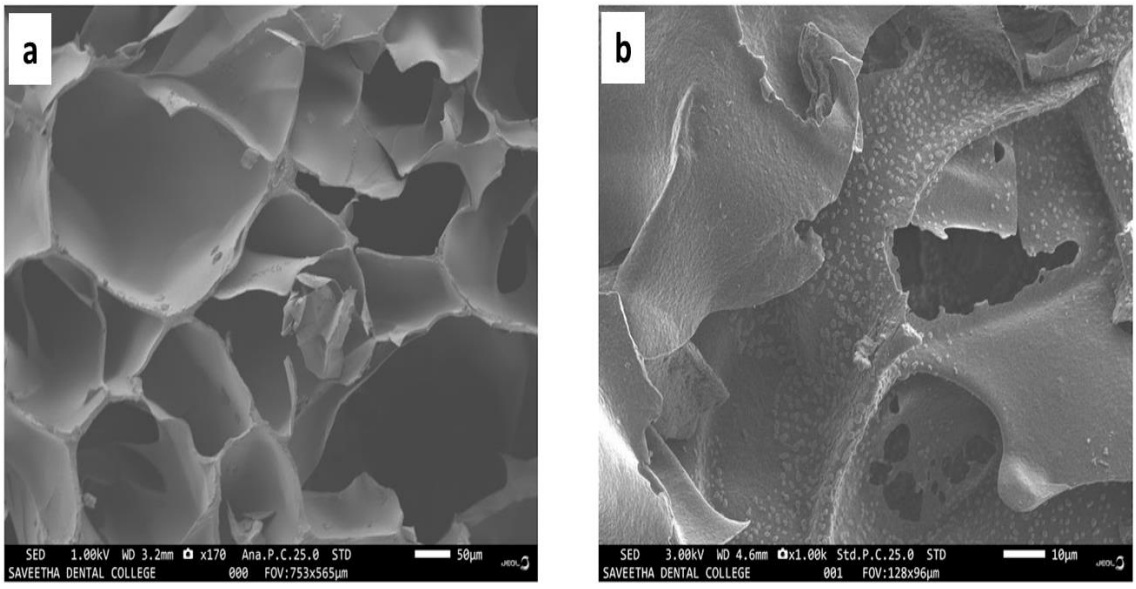

Figure 3. SEM Micrograph of ALG-CHI (a) and ALG-CHI-GO (b) Scaffolds

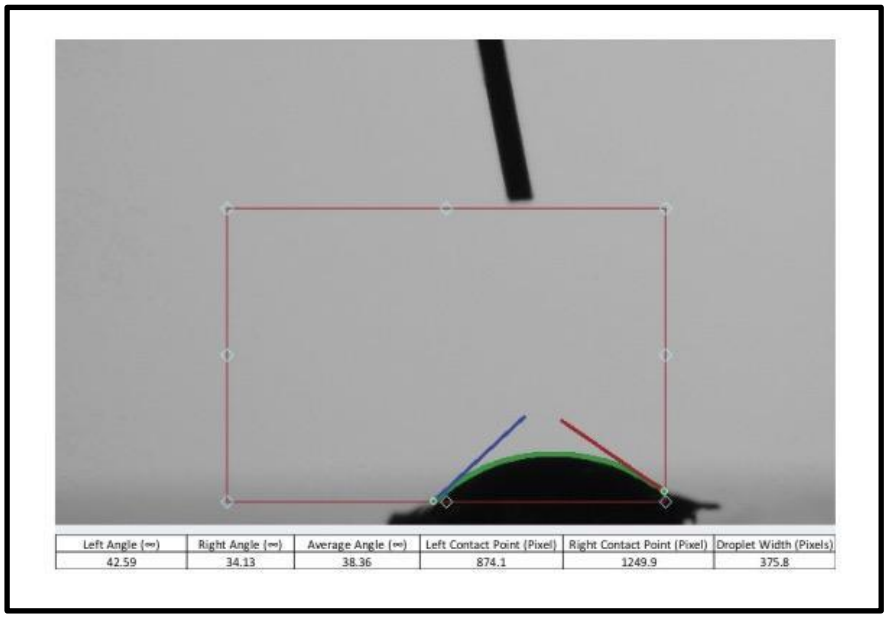

Figure 4. Water Contact Angle of Porous ALG-CHI-GO Scaffold

Antibacterial Activity

Figure 5 represents the antibacterial studies of ALG-CHI-GO scaffold on *Enterococcus faecalis* and *Streptococcus mutans*. It was noted that there was a change in color of the broth medium, post-treatment with the ALG-CHI-GO scaffold. When the ALG-CHI-GO concentration increases, the zone of inhibition of microbes also gradually increases, as the oxygen intake by the organisms decreases, thus proving its antibacterial activity. The minimum inhibitory concentration of E*nterococcus faecalis* and *Streptococcus mutans* was found to be 10 mg/mL.

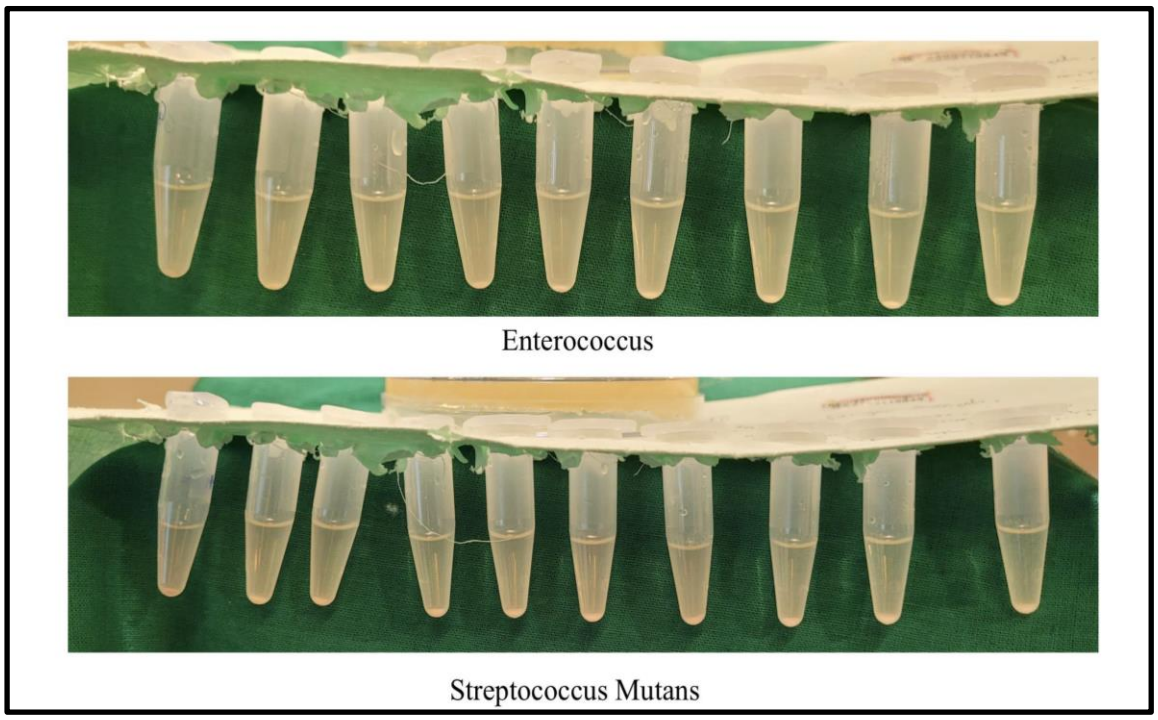

Figure 5. Antibacterial activity of ALG-CHI-GO scaffold on Enterococcus faecalis and Streptococcus Mutans

Annexin V PI Assay

Figure 6 represents the result of Annexin V PI assay of ALG-CHI-GO scaffold. In the current study, the percentage of viable cells was found to be 81.82%, in which the annexin V and PI tend to be in the negative. 18.13% of cells were in the early apoptosis stage, in which the annexin V was positive and PI was negative, 0.05% of cells were in late apoptosis, in which both annexin V and PI were positive. No cells were found to undergo necrosis.

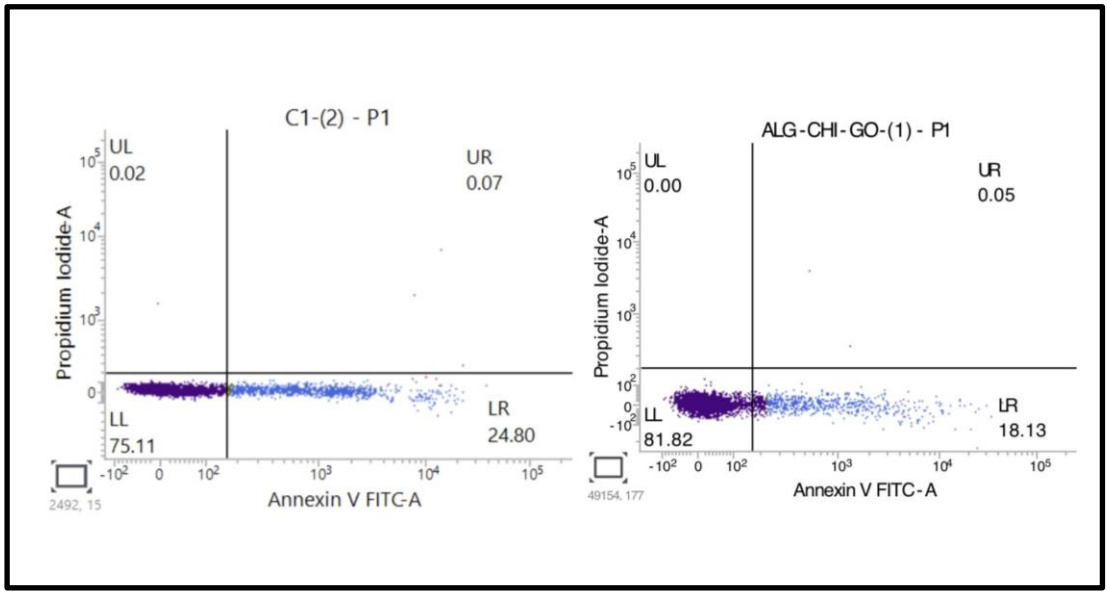

Figure 6. Biocompatibility of ALG-CHI-GO Scaffold

Discussion

Graphene oxide (GO), alginate, and chitosan nanocomposites have gained importance in the medicinal field due to their unique physicochemical properties and biocompatibility. These particles can be fabricated in scaffold forms for better biomedical applications. In our study we have fabricated Graphene oxide-loaded alginate chitosan scaffolds for biomedical applications. Previously, graphene oxide-loaded alginate chitosan collagen scaffolds were reported by [24].

FTIR of ALG-CHI-GO scaffold gave a peak in the fingerprint region of 3500 - 500 cm^{-1} with an intense peak at various regions, indicating the presence of different functional groups; this was concordant with the peak reported in the fabrication of CS/GO/Cur [25]. SEM analysis of ALG-CHI-GO was found to be good compared with the previous report [26]. The water contact angle measurement showed an average angle of 38.36 degrees, indicating the scaffold's hydrophilic nature, which supports cell adherence [27].

The minimum inhibitory concentration of ALG-CHI-GO in E*nterococcus faecalis* and *Streptococcus mutans* was found to be 10 mg/mL in our study. Similar antibacterial studies were reported in composites of chitosan-alginate-AgNPs against *Escherichia coli* and *Staphylococcus aureus.* For Escherichia coli, the zone of inhibition of 11.1 mm, and for Staphylococcus aureus, a zone measuring 10.1 mm [28, 29]. A previous study also reported the antibacterial activity of GO and GO-Ag nanocomposite against Pseudomonas aeruginosa using the conventional counting plate approach. Minimal inhibitory concentration ranged from 2.5 to 5.0 g/mL and GO-Ag nanocomposite demonstrated excellent biocidal activity. These encouraging findings support the notion that GO-Ag nanocomposites may be used as a component of antibacterial coatings [30, 31].

Few studies showed similar results for biocompatibility to our study. One such study stated that utilizing the radiotracer approach and many biological experiments makes it possible to assess the distribution and biocompatibility of graphene oxide (GO) in mice. According to the findings, GO was mostly deposited in the lungs, where it was kept for a very long period. GO had a lengthy blood circulation duration (half-time 5.3 1.2 h) and poor absorption in the reticuloendothelial system compared to other carbon nanomaterials. When mice were exposed to 1 mg/kg body weight of GO for 14 days, no pathological alterations were seen in the tested organs. Additionally, GO demonstrated excellent biocompatibility with red blood cells. According to these findings, GO may be a potential material for medicinal applications, particularly for targeted medication delivery to the lung [19, 32]. Based on all the above analysis, ALG-CHI-GO scaffold is ideal for application in the biomedical field, but further studies are needed to confirm its action more accurately.

Conclusion

In this study, we have successfully fabricated the ALG-CHI-GO scaffold. The results showed that the prepared scaffold (Graphene oxide loaded alginate chitosan scaffold) was found to have antibacterial activities and was biocompatible. This scaffold may have great potential in biomedical fields and be useful. However, in vivo research should be done before using the same for various applications.

Conflicts of Interest

The author declares that there is no conflict of interest.

Authors Contribution

Katheeja Rilah: Literature Search, Experimental, Data Collection, Gayathri R: Analysis, Manuscript Review, Vishnu Priya Veeraraghavan: Study Design, Data Verification, Manuscript Review.

References

[1] Yu, J. R., Navarro, J., Coburn, J. C., Mahadik, B., Molnar, J., Holmes, J. H., and Fisher, J. P. 2019. Current and Future Perspectives on Skin Tissue Engineering: Key Features of Biomedical Research, Translational Assessment, and Clinical Application. *Advanced healthcare materials*, *8*(5): e1801471.

[2] John, S., Kesting, M. R., Paulitschke, P., Stöckelhuber, M., and von Bomhard, A. 2019. Development of a tissue-engineered skin substitute on a base of human amniotic membrane. *Journal of tissue engineering*, *10*: 2041731418825378.

[3] Shi, Q., Luo, X., Huang, Z., Midgley, A. C., Wang, B., Liu, R., and Wang, K. 2019. Cobalt-mediated multi-functional dressings promote bacteria-infected wound healing. *Acta biomaterialia*, *86*: 465–479.

[4] Ren, X., Han, Y., Wang, J., Jiang, Y., Yi, Z., Xu, H., and Ke, Q. 2018. An aligned porous electrospun fibrous membrane with controlled drug delivery - An efficient strategy to accelerate diabetic wound healing with improved angiogenesis. *Acta biomaterialia*, *70*: 140–153.

[5] Giuri, D., Barbalinardo, M., Sotgiu, G., Zamboni, R., Nocchetti, M., Donnadio, A., and Aluigi, A. 2019. Nano-hybrid electrospun non-woven mats made of wool keratin and hydrotalcites as potential bio-active wound dressings. *Nanoscale*, *11*(13): 6422–6430.

[6] Gao, S., Tang, G., Hua, D., Xiong, R., Han, J., Jiang, S., and Huang, C. 2019. Stimuli-responsive bio-based polymeric systems and their applications. *Journal of materials chemistry. B, Materials for biology and medicine*, *7*(5): 709–729.

[7] Ding, Q., Xu, X., Yue, Y., Mei, C., Huang, C., Jiang, S., and Han, J. 2018. Nanocellulose-Mediated Electroconductive Self-Healing Hydrogels with High Strength, Plasticity, Viscoelasticity, Stretchability, and Biocompatibility toward Multifunctional Applications. *ACS applied materials & interfaces*, *10*(33): 27987–28002.

[8] Monica, K., Rajeshkumar, S., Ramasubramanian, A., Ramani, P., and Sukumaran, G. 2022. Anti-inflammatory and antimicrobial effects of herbal formulation using karpooravalli, mint, and cinnamon on wound pathogens. *Journal of advanced pharmaceutical technology & research*, *13*(Suppl 2): S369–S373.

[9] Duraisamy, R., Ganapathy, D., and Shanmugam, R. 2021. Applications of chitosan in dental implantology - A literature review. *International journal of dentistry and oral science*, *8*(9): 4140–4146.

[10] Tan, Q., Tang, H., Hu, J., Hu, Y., Zhou, X., Tao, Y., and Wu, Z. 2011. Controlled release of chitosan/heparin nanoparticle-delivered VEGF enhances regeneration of decellularized tissue-engineered scaffolds. *International journal of nanomedicine*, *6*: 929–942.

[11] Rahmani Del Bakhshayesh, A., Annabi, N., Khalilov, R., Akbarzadeh, A., Samiei, M., Alizadeh, E., and Montaseri, A. 2018. Recent advances on biomedical applications of scaffolds in wound healing and dermal tissue engineering. *Artificial cells, nanomedicine, and biotechnology*, *46*(4): 691–705.

[12] Rubio-Elizalde, I., Bernáldez-Sarabia, J., Moreno-Ulloa, A., Vilanova, C., Juárez, P., Licea-Navarro, A., & Castro-Ceseña, A. B. 2019. Scaffolds based on alginate-PEG methyl ether methacrylate-Moringa oleifera-Aloe vera for wound healing applications. *Carbohydrate polymers*, *206*: 455–467.

[13] Mao, W., Kang, M. K., Shin, J. U., Son, Y. J., Kim, H. S., and Yoo, H. S. 2018. Coaxial Hydro-Nanofibrils for Self-Assembly of Cell Sheets Producing Skin Bilayers. *ACS applied materials & interfaces*, *10*(50): 43503–43511.

[14] Chung, T. W., Yang, J., Akaike, T., Cho, K. Y., Nah, J. W., Kim, S. I., and Cho, C. S. (2002). Preparation of alginate/galactosylated chitosan scaffold for hepatocyte attachment. *Biomaterials*, *23*(14): 2827–2834.

[15] Duraisamy, R., Ganapathy, D., and Shanmugam, R. 2021. Nanocomposites Used In Prosthodontics And Implantology - A Review. *International journal of dentistry and oral science*, *8*(9): 4380–4387.

[16] Ng, I. M. J., and Shamsi, S. 2022. Graphene Oxide (GO): A Promising Nanomaterial against Infectious Diseases Caused by Multidrug-Resistant Bacteria. *International journal of molecular sciences*, *23*(16): 9096.

[17] Balakrishnan, B., Soman, D., Payanam, U., Laurent, A., Labarre, D., and Jayakrishnan, A. 2017. A novel injectable tissue adhesive based on oxidized dextran and chitosan. (2017). *Acta biomaterialia*, *53*: 343–354.

[18] Ravichandran, V., and Jayakrishnan, A. 2018. Synthesis and evaluation of anti-fungal activities of sodium alginate-amphotericin B conjugates. *International journal of biological macromolecules*, *108*: 1101–1109.

[19] Aiswarriya, G. R., Gayathri, R., Veeraraghavan, V. P., Sankaran, K., and Francis, A. P. 2023. Green synthesis, characterization and biocompatibility study of quercetin-functionalized biogenic silver nanoparticles. *Nano*, *18*(7): 2350055.

[20] Paxton, N. C., and Woodruff, M. A. 2022. Measuring contact angles on hydrophilic porous scaffolds by implementing a novel raised platform approach: A technical note. *Polymers for advanced technologies*, *33*(10): 3759–3765.

[21] Ganesh, P. S., and Rai, V. R. 2015. Evaluation of Anti-bacterial and Anti-quorum Sensing Potential of Essential Oils Extracted by Supercritical CO_2 Method Against Pseudomonas aeruginosa. *Journal of Essential Oil Bearing Plants*, *18*(2): 264–275.

[22] Balaganesh, S., Kumar, P., Girija, A. S. S., and Rathinavelu, P. K. 2022. Probiotic curd as antibacterial agent against pathogens causing oral deformities - microbiological study. *Journal of advanced pharmaceutical technology & research*, *13*(Suppl 2): S510–S513.

[23] Tamanna, I. S., Gayathri, R., Sankaran, K., Veeraraghavan, V. P., and Francis, A. P. (2023). Eco-friendly Synthesis of Selenium Nanoparticles Using Orthosiphon stamineus Leaf Extract and Its Biocompatibility Studies. *BioNanoScience*, 1–8 .https://doi.org/10.1007/s12668-023-01277-w

[24] Kolanthai, E., Sindu, P. A., Khajuria, D. K., Veerla, S. C., Kuppuswamy, D., Catalani, L. H., and Mahapatra, D. R. 2018. Graphene Oxide-A Tool for the Preparation of Chemically Crosslinking Free Alginate-Chitosan-Collagen Scaffolds for Bone Tissue Engineering. *ACS applied materials &*

interfaces, *10*(15): 12441–12452.

[25] Nowroozi, N., Faraji, S., Nouralishahi, A., and Shahrousvand, M. 2021. Biological and structural properties of graphene oxide/curcumin nanocomposite incorporated chitosan as a scaffold for wound healing application. *Life sciences*, *264*: 118640.

[26] G., Y. D., V., Prabhu, A., Anil, S., and Venkatesan, J. 2021. Preparation and characterization of dexamethasone-loaded sodium alginate-graphene oxide microspheres for bone tissue engineering. *Journal of drug delivery science and technology*, *64*: 102624.

[27] Zhang, J., Li, J., Jia, G., Jiang, Y., Liu, Q., Yang, X., and Pan, S. 2017. Improving osteogenesis of PLGA/HA porous scaffolds based on dual delivery of BMP-2 and IGF-1*via*a polydopamine coating. *RSC advances*, *7*(89): 56732–56742.

[28] Venkatesan, J., Lee, J.-Y., Kang, D. S., Anil, S., Kim, S.-K., Shim, M. S., and Kim, D. G. 2017. Antimicrobial and anticancer activities of porous chitosan-alginate biosynthesized silver nanoparticles. *International journal of biological macromolecules*, *98*: 515–525.

[29] Sneka, and Santhakumar, P. 2021. Antibacterial Activity of Selenium Nanoparticles extracted from Capparis decidua against Escherichia coli and Lactobacillus Species. *Journal of advanced pharmaceutical technology & research*, *14(8)*: 4452–4454.

[30] de Faria, A. F., Martinez, D. S. T., Meira, S. M. M., de Moraes, A. C. M., Brandelli, A., Filho, A. G. S., and Alves, O. L. 2014. Anti-adhesion and antibacterial activity of silver nanoparticles supported on graphene oxide sheets. *Colloids and surfaces. B, Biointerfaces*, *113*: 115–124.

[31] Anandhi, P., Tharani, M., Rajeshkumar, S., and Lakshmi, T. (2022). Antibacterial activity of cinnamon and clove oil against wound pathogens. *Journal of population therapeutics and clinical pharmacology*, *28*(2): e41–e46.

[32] Kiew, S. F., Kiew, L. V., Lee, H. B., Imae, T., and Chung, L. Y. (2016). Assessing biocompatibility of graphene oxide-based nanocarriers: A review. *Journal of controlled release*, *226*, 217–228.